Materials and Methods

Animal Models. Mice were bred and maintained at the Washington University School of Medicine and all experimental procedures were done in accordance with the animal use oversight committee. Mouse strains utilized included Rosa26-td [1], Rosa26-YFP [2], Flt3-Cre [3], CX3CR1^{ertCre} [4], CCR2^{GFP} [5],CD169-DTR [6], CCR2-DTR [7], Myd88^{flox} [8], LysM-Cre [9], Zbtb46^{GFP} [10] and Tnnt2-DTR. All mice were on the C57/B6 background and genotyped according to established protocols. Equal numbers of male and female mice were included in all experiments. To generate Tnnt2-DTR mice, the rat Tnnt2 promotor (-500 bp) was subcloned into pTRECK6 (kind gift from Dr. Bin Zhou). pTRECK6 contains a multicloning site followed by the β–globin intron and modified version of the human HB-EGF cDNA harboring I117V and L148V mutations. HB-EGF I117V/L148V lacks capacity to signal via epidermal growth factor receptor but retains sensitivity to Diphtheria toxin (DT). pTRECK6 was a kind gift from Kenji Kohno. Linearized plasmid was injected in C57/CBA blastocysts and transferred into pseudo-pregnant mice. Founders were then identified by PCR and screened by western blot and immunohistochemistry for selective expression of HB-EGF (R&D cat# AF-259-NA) in the heart. Suitable Tnnt2-DTR founder animals were crossed to C57/B6 mice for 3 generations prior to performing experiments. Cardiomyocyte injury was induced by administering 25 ng diphtheria toxin (Sigma) via intraperitoneal injection to Tnnt2-DTR transgenic mice.

Heart Transplantation. Heart grafts were harvested from wild type, CCR2-DTR, CD169-DTR, Flt3-Cre Rosa26-tdTomato or Myd88^{flox} LysM-Cre mice on a C57/B6 background were transplanted into the right neck of Flt3-Cre Rosa26-YFP, CD45.1 or CCR2–GFP recipients following 1 hour of cold (4°C) ischemia as previously described [11]. The recipient right common carotid artery and right external jugular vein were connected via cuff technique to the donor

ascending aorta and the donor pulmonary artery, respectively. Grafts resumed a regular heartbeat immediately following reperfusion.

Intravital 2-photon microscopy. Time-lapse imaging was performed with a custom-built 2-photon microscope running ImageWarp version 2.1 acquisition software (A&B Software). 4 hours after reperfusion, CCR2-GFP recipient mice were anesthetized with an i.p. injection of ketamine (80 mg/kg) and xylazine (10 mg/kg) and maintained with halved doses administered every hour. Mice were intubated orotracheally with a 20-gauge angiocatheter and ventilated with room air at a rate of 120 breaths per minute and with a tidal volume of 0.5 ml. For time-lapse imaging of monocytes migration in heart grafts, we averaged 15 video-rate frames (0.5 seconds per slice) during the acquisition to match the ventilator rate and minimize movement artifacts. Each plane represents an image of 220 × 240 μm in the x and y dimensions. Twenty-one sequential planes were acquired in the z dimension (2.5 μm each) to form a Z stack. Each individual monocyte was tracked from its first appearance in the imaging window and followed up to the time point at which it dislocated more than 20 μm from its starting position. To determine the percentage of extravasated monocytes, we divided the number of extravascular monocytes by the sum of intravascular and extravascular monocytes. In 50 μl of PBS, 20 μl of 655-nm nontargeted Q-dots were injected i.v. to visualize blood vessels. Two-photon excitation produced a second harmonic signal from collagen within the myocardial tissue. Multidimensional rendering and manual cell tracking was done with Imaris (Bitplane). Data were transferred and plotted in GraphPad Prism 6.0 (Sun Microsystems Inc.) for creation of the graphs.

Reperfusion myocardial infarction (ischemia reperfusion injury) and permanent myocardial infarction (LAD Ligation). For closed-chest ischemia reperfusion injury, two to four month old mice on the C57/B6 background were anesthetized with sodium pentobarbital,

intubated, and mechanically ventilated. A midline incision was made to expose the heart and an 8-0 prolene suture was then placed around the proximal left coronary artery to maximize the ischemic area. The suture was then threaded through a 1 mm piece of polyethylene tubing forming a loose snare to serve as the arterial occluder. Each end of the suture was exteriorized through the thorax and stored in a subcutaneous pocket. The skin was then closed over the exteriorized suture ends with 5-0 prolene suture. Instrumented mice were allowed to recover for 2 weeks prior to induction of ischemia. Ischemia was induced after anesthetizing the animals with inhaled 1.5% isoflurane. The skin was opened over the subcutaneous pocket and exposing the exteriorized suture. The suture ends were dissected away from the subcutaneous tissue and tension was exerted until ST-segment elevation was seen on the ECG. Ischemia was confirmed by visualizing wall motion abnormality using simultaneous echocardiography. Following 90 minutes of ischemia time, tension was released and the suture ends were placed back into the subcutaneous pocket. The skin was then closed as described above. Sham animals underwent the identical procedure with the exception that tension was not placed on the suture ends.

For coronary artery ligation, mice were anesthetized with ketamine (100 mg/kg) and xylazine (10 mg/kg) administered i.p. Mice were restrained supine, intubated, and ventilated. A left thoracotomy was performed, the LV and the left main coronary artery system exposed, and the left anterior descending coronary artery (LAD) ligated with a 9-0 silk suture. The surgical incision was closed and the mice were recovered on a warmer until being returned to their cage. All cardiovascular physiological studies were performed in accordance with recommended guidelines[12, 13, 14].

Parabiosis. Female donor and recipient mice were shaved and matching skin incisions were made from behind the ear to the tail of each mouse. The subcutaneous fascia was dissected to create a free skin flap. The olecranon and knee joints were anastomosed using mono-nylon 5.0

suture (Ethicon) and skin flaps anastomosed using a continuous suture. Postoperative anesthesia included 0.1mg/kg injection of buprenorphine administered subcutaneously after surgery and 24 hours later. 3% neomycin was administered for 2 weeks. Mice were analyzed at 3 and 6 weeks following surgery. The percentage chimerism for each macrophage subset was normalized to blood monocyte chimerism in the recipient mouse.

Echocardiography. Mouse echocardiography was performed in the Washington University Mouse Cardiovascular Phenotyping Core facility using the VisualSonics 770 Echocardiography System. Avertin (0.005 ml/g) was used for sedation based on previously established methods of infarct quantification [15]. 2D and M-mode images were obtained in the long and short axis views. Ejection fraction (EF) and LV dimensions were calculated using edge detection software and standard techniques. The akinetic region was calculated by measuring the area of the akinetic portion of the LV myocardium and normalizing it to the area of the total LV myocardium. Measurements were performed on 3 independently acquired images per animal, by investigators who were blinded to experimental group. Each experimental group included at least 5 animals.

Triphenyltetrazolium chloride (TTC) staining. Hearts were harvested from mice 48 hours following ischemia reperfusion injury, perfused with 20ml of ice cold PBS, and sliced into 4 pieces using a razor blade. Myocardial slices were then immersed in 1% TTC (Sigma) diluted in 0.9% sodium chloride and incubated from 30 minutes on an agitator at 37C. Slices were then fixed in 10% formalin and images on a Zeiss stereomicroscope. Quantification of infract area was performed using ImageJ software in blinded fashion.

Flow cytometry. Single cell suspensions were generated from saline perfused hearts by finely mincing and digesting them in DMEM with Collagenase 1 (450 U/ml), Hyaluronidase (60 U/ml)

and DNase I (60 U/ml) for 1 hour at 37°C. All enzymes were purchased from Sigma. To deactivate the enzymes samples were washed with HBSS that was supplemented with 2% FBS and 0.2% BSA and filtered through 40 μM cell strainers. Red blood cell lysis was performed with ACK lysis buffer (Thermo Fisher Scientific). Samples were washed with HBSS and resuspended in 100 μL of FACS buffer (DPBS with 2% FBS and 2 mM EDTA). Cells were stained with monoclonal antibodies at 4°C for 30 minutes in the dark. All the antibodies were obtained from Biolegend. A complete list of antibodies is provided below. Samples were washed twice, and final resuspension was made in 300 μL FACS buffer. DAPI or LIVE/DEADTM Aqua dyes were used for exclusion of dead cells. Immune cells were first gated as CD45+. Neutrophils were gated as $Ly6G^{high}CD64$-. Monocytes were gated as $CD64^{int}Ly6C^{high}$ CCR2+ $MHCII^{low}$. Macrophages were gated as Ly6G-$CD64^{high}Ly6C^{low}$ cells. T-cells and B-cells were isolated from splenic preparations using CD3e and CD19 as cell surface markers. Flow cytometric analysis and sorting were performed on BD LSRII and BD FACS ARIAIII platforms, respectively.

CD45-PerCP/Cy5.5, clone 30-F11 (Biolegend cat# 103131)

CD64-APC and PE, clone X54-5/7.1 (Biolegend cat# 139305, 139303)

CCR2-BV421, clone: SA203G11 (Biolegend cat# 150605)

MHCII-APC/Cy7, clone M5/114.15.2 (Biolegend cat# 107627)

Ly6G-PE/Cy7, clone 1A8 (Biolegend cat# 127617)

Ly6C-APC and FITC, clone HK1.4 (Biolegend cat# 128015, 128005)

CD45.1-PE, clone A20 (Biolegend cat# 110707)

CD45.2-PerCP/Cy5.5, clone 104 (Biolegend cat# 109827)

CD3e-APC, clone 145-2C11 (Biolegend cat# 100311)

CD19-PE, clone 6D5 (Biolegend cat# 115507)

Pulse chase tracking of resident cardiac macrophages. To label cardiac resident macrophages, tamoxifen inducible Tnnt2-DTR CX_3CR1^{ertCre} Rosa26-tdTomato reporter mice were used. Tamoxifen food pellets (500 mg per kg diet, Envigo Teklad Diets, Madison WI) were made available ad libitum for two weeks for the pulse phase. This period allowed for activation of the Cre recombinase and labeling of tissue resident macrophages and circulating (bone marrow derived) monocytes with the tdTomato reporter. Mice were then given regular chow ad libitum for two weeks. After the chase phase, resident cardiac macrophages (long lived and slow turnover) retained the tdTomato labeling while circulating monocytes were unlabeled owing to their high turnover and shorter half-life.

Macrophage Depletion Strategies. To deplete resident CCR2- or CCR2+ macrophages prior to heart transplantation, donor mice (control, CD169-DTR, or CCR2-DTR) were administered diphtheria toxin (Sigma) 100ng IP daily for 4 days prior to transplantation. To deplete resident CCR2- macrophages prior to ischemia reperfusion injury, control or CD169-DTR mice were treated with diphtheria toxin (Sigma) 100ng IP daily for 7 days prior to transplantation. To deplete resident CCR2+ macrophages prior to ischemia reperfusion injury, control or CCR2-DTR mice were treated with a single dose of diphtheria toxin (Sigma) 100ng IP 4 days prior to ischemia reperfusion injury. Immediately after diphtheria toxin treatment, both CCR2+ monocytes and CCR2+ macrophages were depleted. However, 4 days following diphtheria toxin treatment, CCR2+ monocytes were repopulated whereas resident CCR2+ macrophages remained depleted.

Immunostaining, Picrosirius Red, Wheat Germ Agglutinin, and Ethidium Homodimer-1 Staining. For histological analyses, tissues were fixed in 2% PFA overnight at 4°C, dehydrated in 70% ethyl alcohol, and embedded in paraffin. 4-μm sections were cut and stained with Picrosirius red using standard techniques. Picrosirius red staining was quantified using Image J

software. For all immunostaining assays tissues were fixed in 2% PFA overnight at 4°C, embedded in OCT, infiltrated with 30% sucrose, frozen, and 12-µm cryosections cut. Primary antibodies used were: CD68 cone FA-11 1:400 (Biolegend cat# 137001), Ly6G clone 1A8 1:100 (BD cat# 551459), Arginase-1 clone D4E3M 1:200 (Cell Signaling cat# 93668), LYVE1 1:200 ab14917 (Abcam cat# ab93668), CD13 clone R3-63 1:200 (Bio Rad cat# MCA2183), Integrin B7 clone 2G18 1:200 (Novus cat# Nb110-94147), and CD64 AF2074 1:100 (R&D cat# AF2074). Immunofluorescence was visualized using appropriate secondary antibodies on a Zeiss confocal microscopy system. To quantify cardiomyocyte cross-sectional area paraffin sections were stained with rhodamine conjugated WGA (Vector labs), visualized on a Zeiss confocal microscope, and measurements preformed using Zeiss Axiovision software. Ethidium homodimer-1 staining was injected IV immediately after heart transplantation. Hearts were then harvested 2 hours after ethidium homodimer injection and fixed in 2% PFA. Ethidium homodimer staining as visualized on cryosections using a Zeiss confocal microscope. For all experiments, at least 4 sections from 4 independent samples were analyzed in blinded fashion.

RNA sequencing. Hearts were harvested at day 0, day 2, and day 4 following DT injection (25ng IP) into Tnnt2-DTR;CCR2-GFP;Flt3Cre-Rosa26-tdTomato mice. Single cell suspensions were generated from the hearts as described in the flow cytometry section. Cells were stained with CD45, CD64, Ly6C, MHCII, Ly6G monoclonal antibodies. LIVE/DEAD^{TM} Aqua dye was used for exclusion of dead cells. Immune cells were first gated as CD45+. Monocytes were gated as CD64^{int}Ly6C^{high}GFP+MHCII^{low}. Macrophage subpopulations were gated as CD64^{high}Ly6C^{low}MHCII^{high} GFP+Flt3$^{dtomato+}$, CD64^{high}Ly6C^{low}MHCII^{high} GFP-Flt3$^{dtomato-}$, and CD64^{high}Ly6C^{low}MHCII^{high} GFP-Flt3$^{dtomato+}$ populations. Sorting was performed on BD FACS ARIA III platform with 85 µM nozzle and flow rate set to 1 µl/min. All populations were double sorted to ensure >99% purity. Sample collection holder was set at 4 degree Celsius. A total of 1000 cells were sorted for each population directly into the 5 µl of TCL lysis buffer (Qaigen)

containing 1% BME. Samples were then sent to the ImmGen consortium and subjected to library construction and sequencing. Sequence alignment and quantitation was performed by the ImmGen [16]. Differential gene expression was performed using STAR [17] and Partek analysis packages.

RT-PCR

RNA was extracted from sorted cells or myocardial tissue using the RNeasy RNA mini kit and Tissue Lyser II (Qiagen). RNA concentration was measured using a nanodrop spectrophotometer (ThermoFisher Scientific). cDNA synthesis was performed using the High Capacity RNA to cDNA synthesis kit (Applied Biosystems). For sorted macrophages, cDNA was synthesized using the iScript™ Reverse Transcription Supermix (Bio-Rad) and pre-amplified using the Sso Advanced PreAmp Supermix kit (Bio-Rad). Quantitative real time PCR reactions were prepared with sequence-specific primers (IDT) with PowerUP™ Syber Green Master mix (ThermoFisher Scientific) in a 20 µL volume. Real time PCR was performed using QuantStudio 3 (ThermoFisher Scientific). mRNA expression was normalized to 36B4. Primers were purchased from IDT.

Single cell RNA sequencing. cDNA libraries from FACS sorted CD45+CD11b+Ly6G-CD64+ cells were generated using the 10X Genomics platform per manufacturer recommended protocols. Cells were sequenced at a target read depth of 100,000 reads/cell using a HiSeq 4000 sequencer (Illumina). Sequencing alignment and de-multiplexing was performed using Cell Ranger from 10x Genomics. Additional analysis was performed with Seurat [18], using the raw gene counts imported from Cell Ranger. None of the 17,931 cells expressed mitochondrial genes at a rate greater than 5 percent of their total gene expression and therefore no cells were excluded from further analysis. A scale factor of 10000 and log transformation was used to normalize the read counts. Further normalization was achieved by regressing out variation in

the number of reads per cell and percentage of mitochondrial genes expressed. We identified 1452 genes differentially expressed greater than 0.5 standard deviations from the mean and with average expression between 0.0125 and 3 across all cells. Clustering of cells was performed using 10 principal components derived from the differentially expressed genes and identified 9 independent clusters. A heatmap used for cluster identification was generated using the top 10 markers enriched in each cluster by p-value from genes expressed in at least 25 percent of cells in that cluster. Violin and feature plots were generated using Loupe Browser (10X genomics).

Statistical Analysis. Data were analyzed by using software (Prism, version 6.0-7.0; GraphPad, La Jolla, Calif). Differences between groups were compared by using Mann-Whitney U test. Multiple means were compared by using a one- or two-way analysis of variance with the post-hoc Tukey test. $P<0.05$ (two-sided) was indicative of a statistically significant difference. Bonferroni correction was performed when multiple hypotheses were tested. Data are presented as dot plots or box whisker plots generated in PRISM. The exact sample size used to calculate statistical significance is stated in the appropriate figure legend.

Data Availability. Source Data for all experiments have been provided. All other data are available from the corresponding author on reasonable request. Gene expression data will be deposited in GEO at the time of publication. Additional details can be found in the Reporting Checklist.

References

1. Madisen, L. *et al.* A robust and high-throughput Cre reporting and characterization system for the whole mouse brain. *Nat Neurosci* **13**, 133-140 (2010).

2. Srinivas, S. *et al.* Cre reporter strains produced by targeted insertion of EYFP and ECFP into the ROSA26 locus. *BMC Dev Biol* **1**, 4 (2001).

3. Boyer, S.W., Schroeder, A.V., Smith-Berdan, S. & Forsberg, E.C. All hematopoietic cells develop from hematopoietic stem cells through Flk2/Flt3-positive progenitor cells. *Cell Stem Cell* **9**, 64-73 (2011).

4. Yona, S. *et al.* Fate mapping reveals origins and dynamics of monocytes and tissue macrophages under homeostasis. *Immunity* **38**, 79-91 (2013).

5. Satpathy, A.T. *et al.* Notch2-dependent classical dendritic cells orchestrate intestinal immunity to attaching-and-effacing bacterial pathogens. *Nat Immunol* **14**, 937-948 (2013).

6. Miyake, Y. *et al.* Critical role of macrophages in the marginal zone in the suppression of immune responses to apoptotic cell-associated antigens. *J Clin Invest* **117**, 2268-2278 (2007).

7. Hohl, T.M. *et al.* Inflammatory monocytes facilitate adaptive CD4 T cell responses during respiratory fungal infection. *Cell Host Microbe* **6**, 470-481 (2009).

8. Hou, B., Reizis, B. & DeFranco, A.L. Toll-like receptors activate innate and adaptive immunity by using dendritic cell-intrinsic and -extrinsic mechanisms. *Immunity* **29**, 272-282 (2008).

9. Clausen, B.E., Burkhardt, C., Reith, W., Renkawitz, R. & Forster, I. Conditional gene targeting in macrophages and granulocytes using LysMcre mice. *Transgenic Res* **8**, 265-277 (1999).

10. Satpathy, A.T. *et al.* Zbtb46 expression distinguishes classical dendritic cells and their committed progenitors from other immune lineages. *J Exp Med* **209**, 1135-1152 (2012).

11. Li, W. *et al.* Intravital 2-photon imaging of leukocyte trafficking in beating heart. *J Clin Invest* **122**, 2499-2508 (2012).

12. Lindsey, M.L. *et al.* Guidelines for experimental models of myocardial ischemia and infarction. *Am J Physiol Heart Circ Physiol* **314**, H812-H838 (2018).

13. Lindsey, M.L., Gray, G.A., Wood, S.K. & Curran-Everett, D. Statistical considerations in reporting cardiovascular research. *Am J Physiol Heart Circ Physiol* **315**, H303-H313 (2018).

14. Lindsey, M.L., Kassiri, Z., Virag, J.A.I., de Castro Bras, L.E. & Scherrer-Crosbie, M. Guidelines for measuring cardiac physiology in mice. *Am J Physiol Heart Circ Physiol* **314**, H733-H752 (2018).

15. Kanno, S. *et al.* Echocardiographic evaluation of ventricular remodeling in a mouse model of myocardial infarction. *J Am Soc Echocardiogr* **15**, 601-609 (2002).

16. Heng, T.S., Painter, M.W. & Immunological Genome Project, C. The Immunological Genome Project: networks of gene expression in immune cells. *Nat Immunol* **9**, 1091-1094 (2008).

17. Dobin, A. *et al.* STAR: ultrafast universal RNA-seq aligner. *Bioinformatics* **29**, 15-21 (2013).

18. Butler, A., Hoffman, P., Smibert, P., Papalexi, E. & Satija, R. Integrating single-cell transcriptomic data across different conditions, technologies, and species. *Nat Biotechnol* **36**, 411-420 (2018).

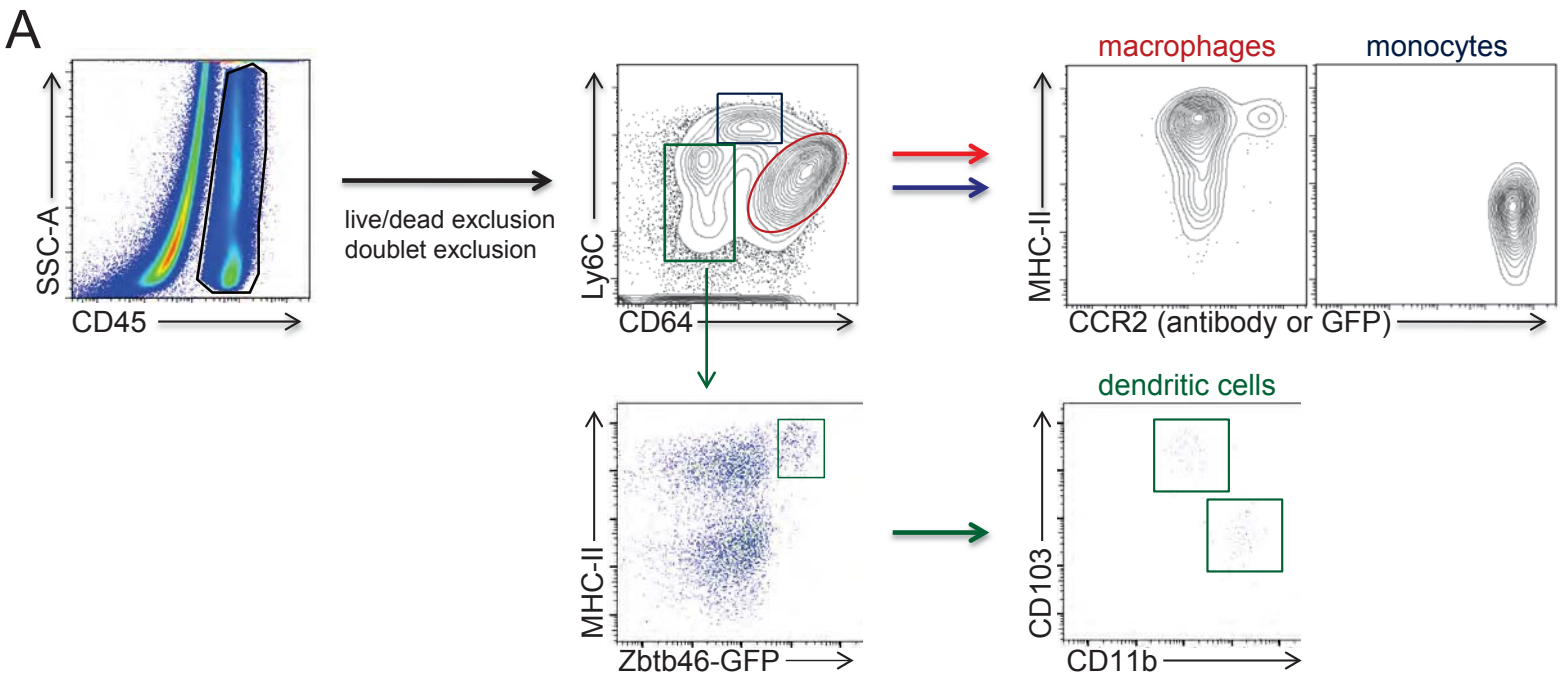
A
SSC-A
CD45
live/dead exclusion
doublet exclusion
Ly6C
CD64
macrophages
monocytes
MHC-II
CCR2 (antibody or GFP)
MHC-II
Zbtb46-GFP
dendritic cells
CD103
CD11b

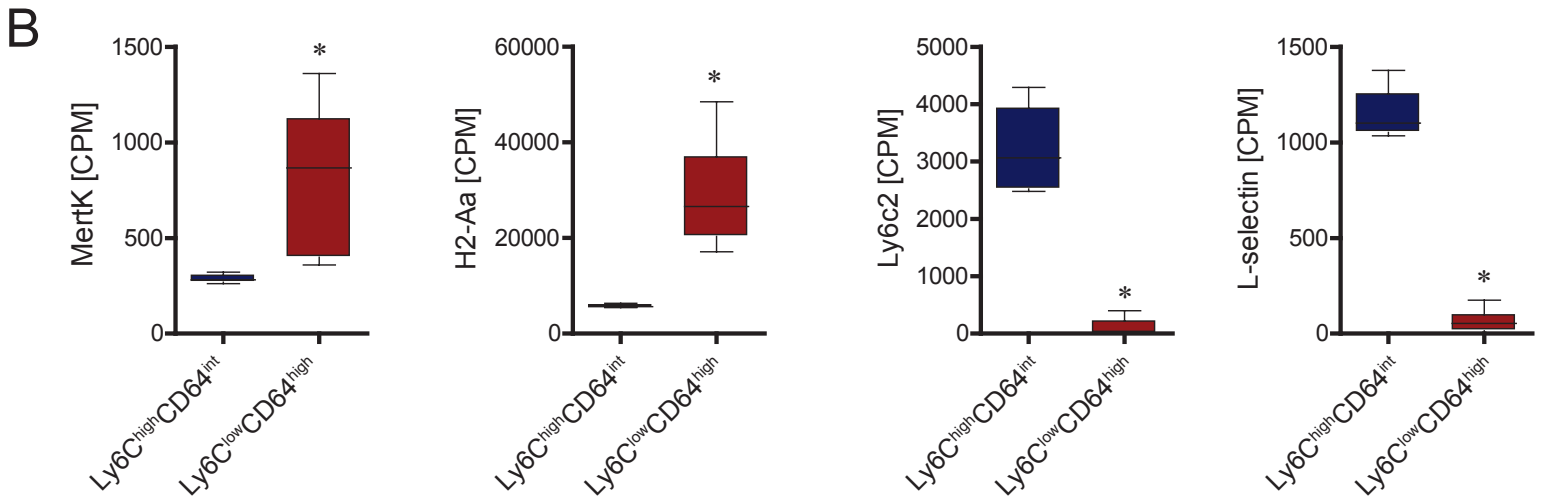
B
MertK [CPM]
H2-Aa [CPM]
Ly6c2 [CPM]
L-selectin [CPM]
Ly6C^high CD64^int
Ly6C^low CD64^high

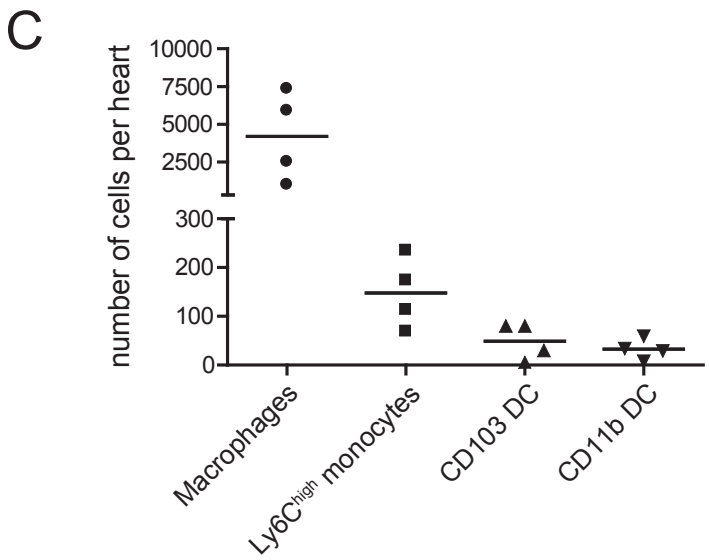
C
number of cells per heart
Macrophages
Ly6C^high monocytes
CD103 DC
CD11b DC

Online Figure I. Monocyte and macrophage flow cytometry gating strategies. A, Gating strategy for cardiac monocyte ($Ly6C^{high}CD64^{int}$), macrophage ($Ly6C^{low}CD64^{high}$), and dendritic cell ($CD64^{-}MHC\text{-}II^{high}Zbtb46^{+}$) populations. **B**, Quantification of RNA sequencing data showing the expression of monocyte (Ly6C2, L-selectin) and macrophage (MertK, H2-Aa) in $Ly6C^{high}CD64^{int}$ monocytes and $Ly6C^{low}CD64^{high}$ macrophages. Data is displayed as box and whisker plots. Line denotes the mean value. *$p<0.05$ compared to other experimental groups. **C**, Quantification of monocytes, macrophages, and dendritic cells in the naïve heart.

A

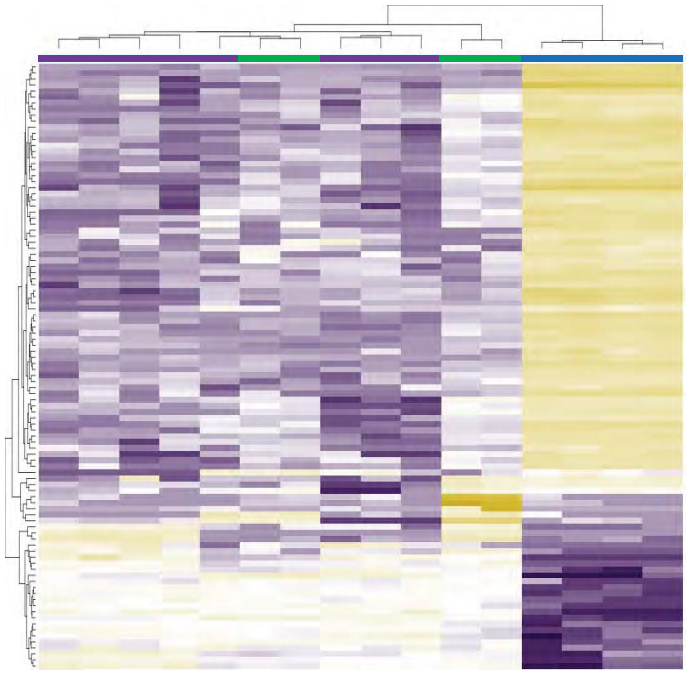

CCR2+ macrophages
CCR2- Flt3-Cre positive macrophages
CCR2- Flt3-Cre negative macrophages

B

GSEA Pathway Analysis

Enriched in CCR2+ macrophages

- TNF and NFkb signaling
- Inflammatory response
- mTORC1 signaling
- Interferon signaling
- IL2 STAT5 signaling
- Hypoxia
- Complement
- Glycolysis
- Allograft rejection
- p53 pathway
- Specific transcripts: CCL5, CCL17, IL1A, IL1B, IL6, TIMP1

Enriched in CCR2- macrophages

- Myogenesis
- UV response DNA damage
- Mitosis
- Epithelial Mesenchymal Transition
- Apical Junction
- K-Ras signaling
- Specific transcripts: IGF1, PDGF-C, HB-EGF, Cyr61 Coll3/4/6

C

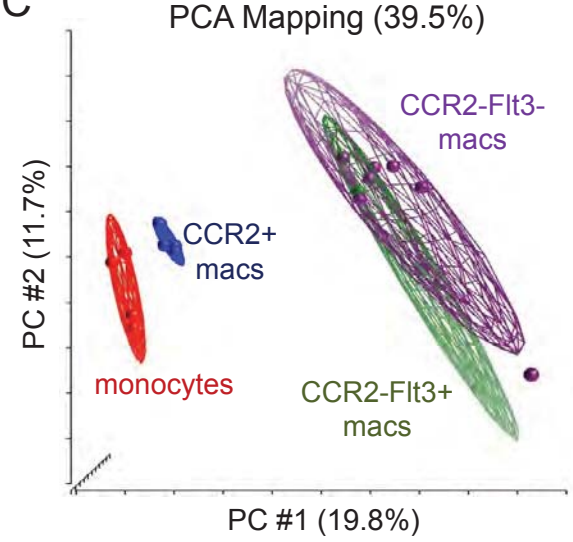

D

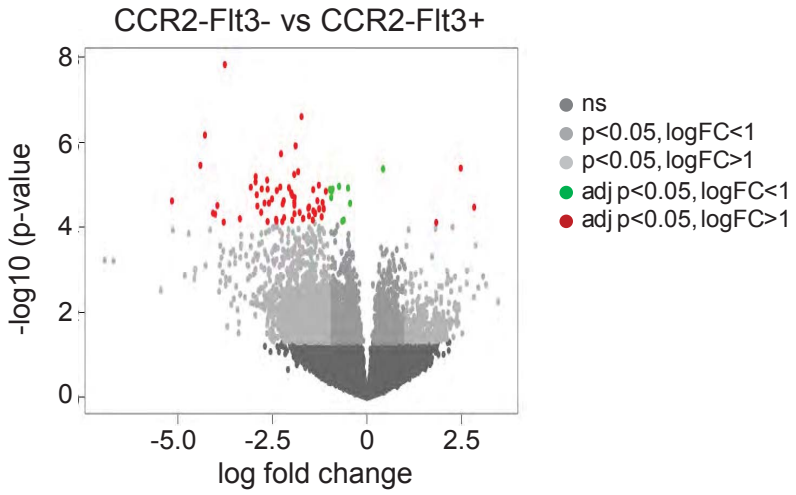

E

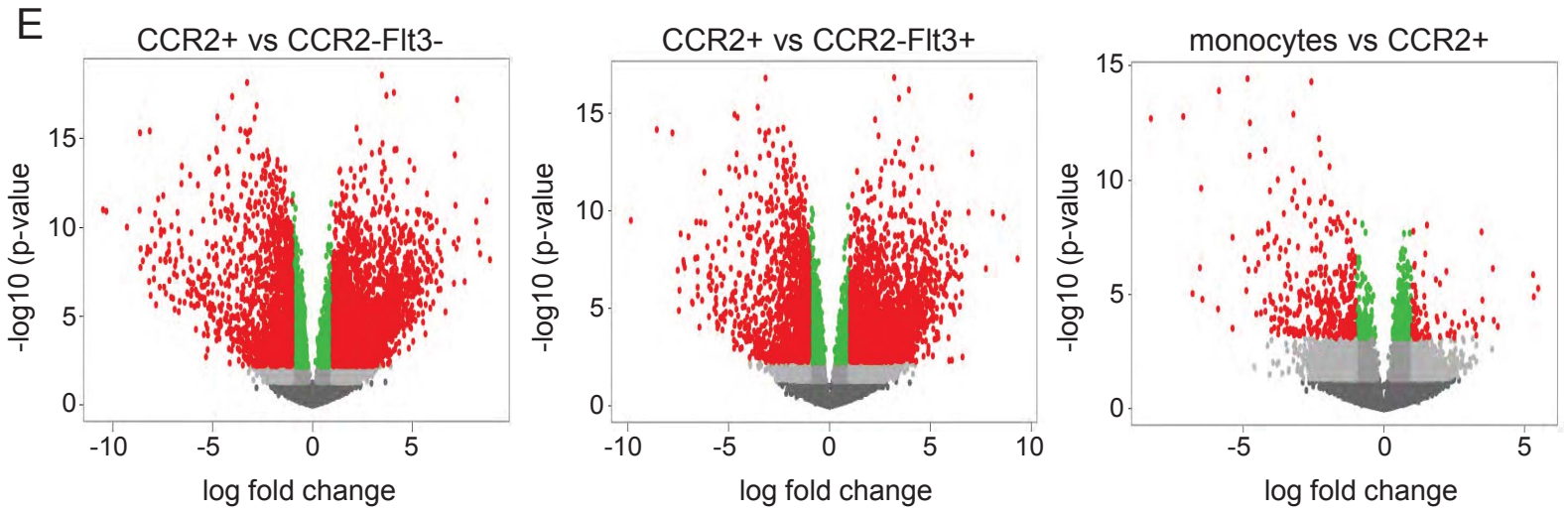

Online Figure II. Transcriptomic characterization of resident macrophage populations. **A,** Hierarchical clustering based on genes differentially expressed between resident CCR2+ macrophages, CCR2- Flt3-Cre negative, and CCR2- Flt3-Cre positive macrophages. **B**, GSEA pathway analysis showing pathways and specific genes enriched in resident CCR2- and CCR+ macrophages. **C**, Principal components analysis showing the relationship between monocytes (red), resident CCR2+ macrophages (blue), resident CCR2- Flt3-Cre negative macrophages (purple), and resident CCR2- Flt3-Cre positive macrophages (green). **D**, Volcano plot showing the number of genes differentially expressed between resident CCR2- Flt3-Cre negative and CCR2- Flt3-Cre positive macrophages. **E**, Volcano plots showing the number of genes differentially expressed between resident CCR2+ versus resident CCR2- Flt3-Cre negative macrophages (left), resident CCR2+ macrophages versus resident CCR2- Flt3-Cre positive macrophages (center) and monocytes versus resident CCR2+ macrophages (right). logFC: log based 2 fold change, adj p: adjusted p-value (FDR analysis).

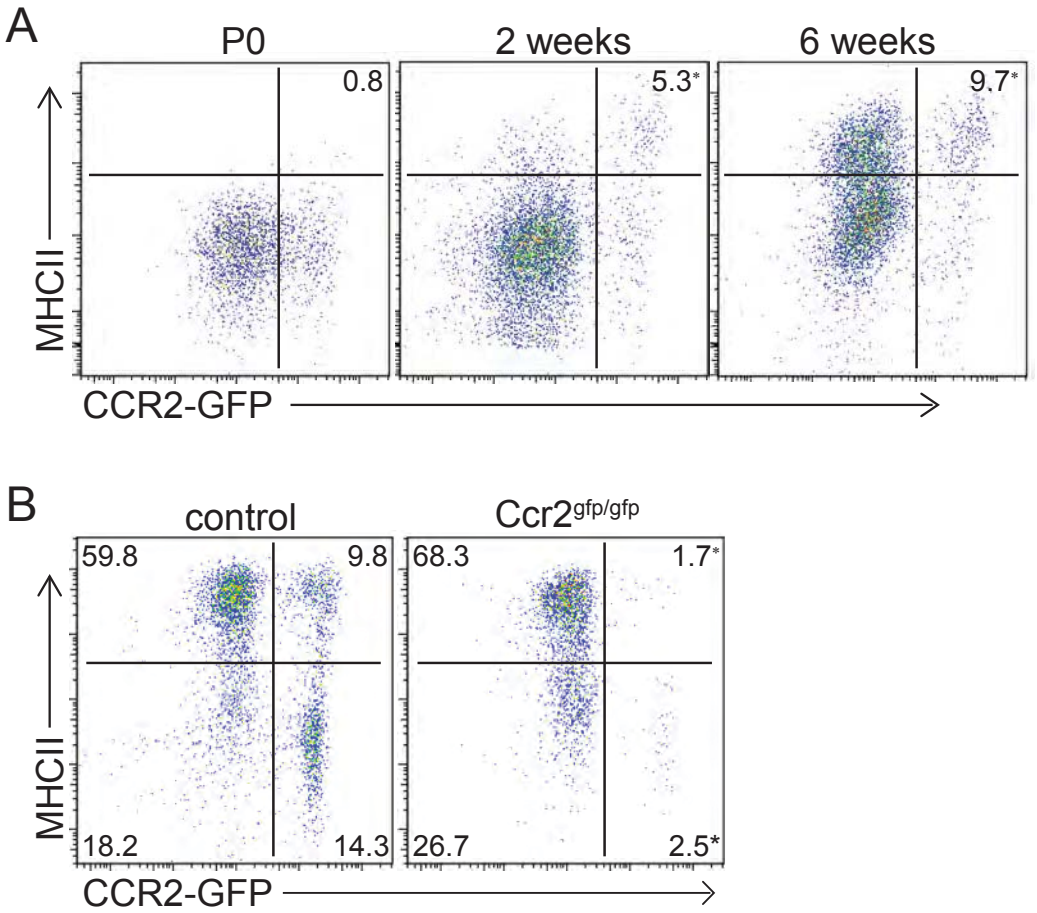
A
P0
2 weeks
6 weeks
0.8
5.3*
9.7*
MHCII
CCR2-GFP
B
control
Ccr2gfp/gfp
59.8
9.8
18.2
14.3
68.3
1.7*
26.7
2.5*
MHCII
CCR2-GFP

Online Figure III. Dynamics of resident CCR2+ macrophages in naïve mice. A, Flow cytometry of cardiac CD45+CD64+ monocytes and macrophages at P0, 2 weeks, and 6 weeks of age. Values displayed indicate the percentage of CD45+CD64+MHC-II^{high}CCR2+ macrophages. *p<0.05 compared to P0. **B**, Flow cytometry of control and Ccr2$^{gfp/gfp}$ hearts at weeks of age. Values displayed indicate the percentage of monocytes or macrophages within each quadrant. *p<0.05 compared to control.

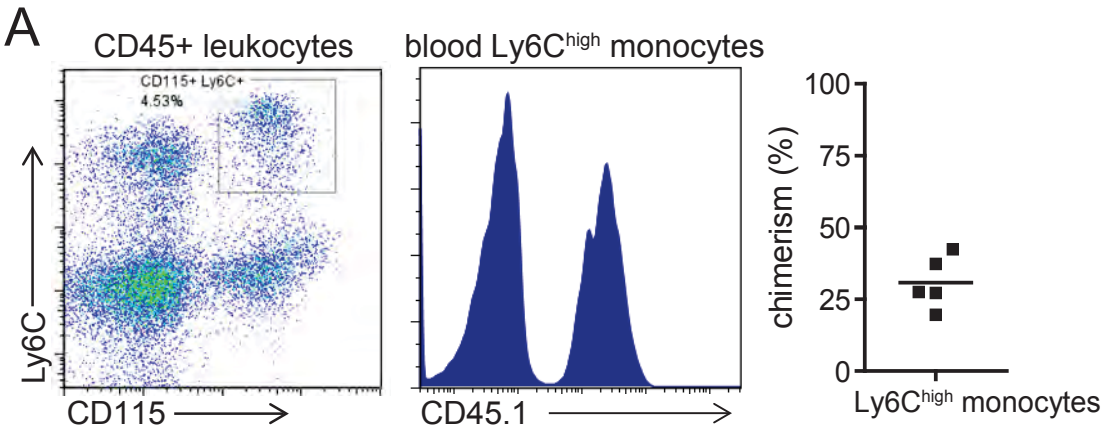
A
CD45+ leukocytes
blood Ly6C^high monocytes
CD115+ Ly6C+
4.53%
Ly6C
CD115
CD45.1
chimerism (%)
100
75
50
25
0
Ly6C^high monocytes

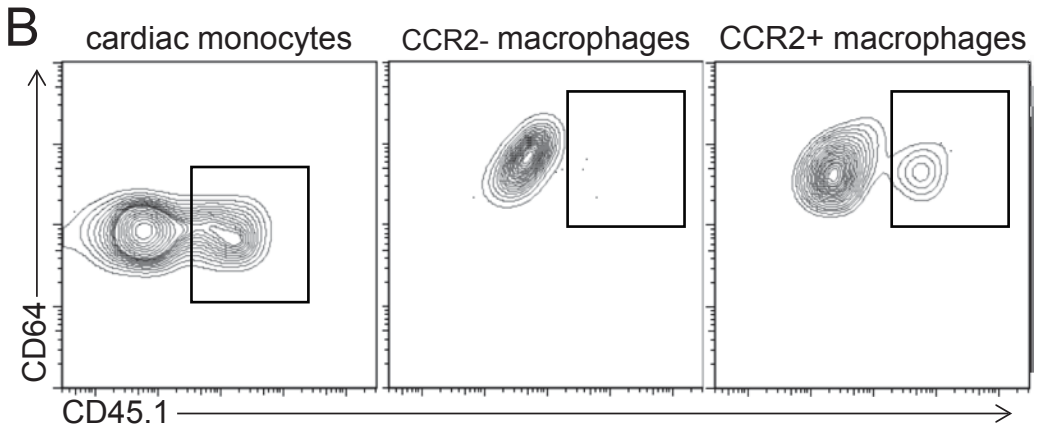
B
cardiac monocytes
CCR2- macrophages
CCR2+ macrophages
CD64
CD45.1

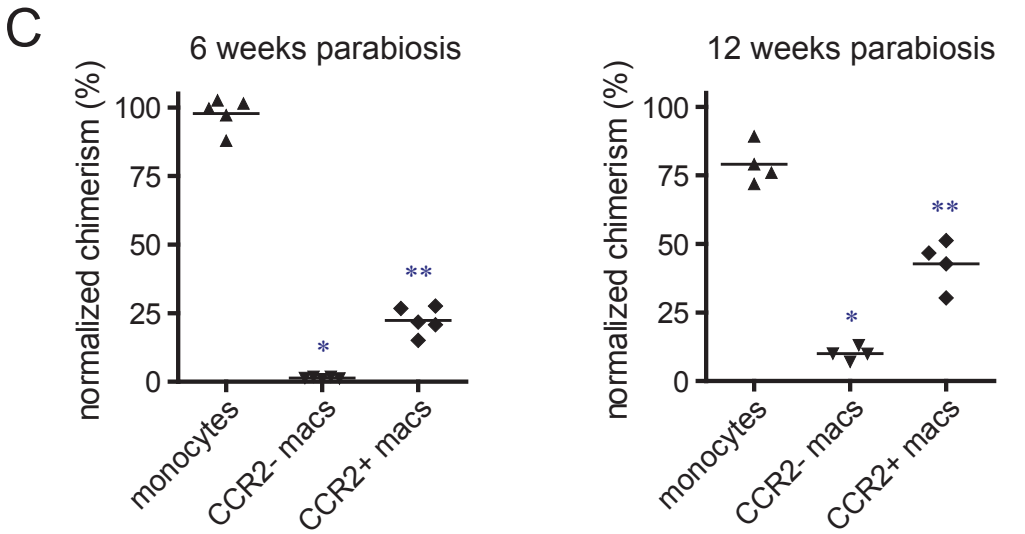
C
6 weeks parabiosis
12 weeks parabiosis
normalized chimerism (%)
100
75
50
25
0
*
**
monocytes
CCR2- macs
CCR2+ macs

Online Figure IV. Dynamics of cardiac monocytes and macrophages in parabiotic mice. **A**, Flow cytometry of peripheral blood monocytes from CD45.1-CD45.2 parabionts showing the percentage of chimerism within Ly6C^{high} monocytes. **B**, Flow cytometry of hearts from CD45.1-CD45.2 parabiotic mice showing the extent of chimerism within cardiac monocyte and macrophage subsets. **C**, Quantification of percent chimerism in cardiac monocytes, CCR2- macrophages, and CCR2+ macrophages after 6 and 12 weeks of parabiosis. Data is normalized to peripheral Ly6C^{high} monocyte chimerism. *$p<0.05$ compared to monocytes. **$p<0.05$ compared to monocytes and CCR2- macrophages.

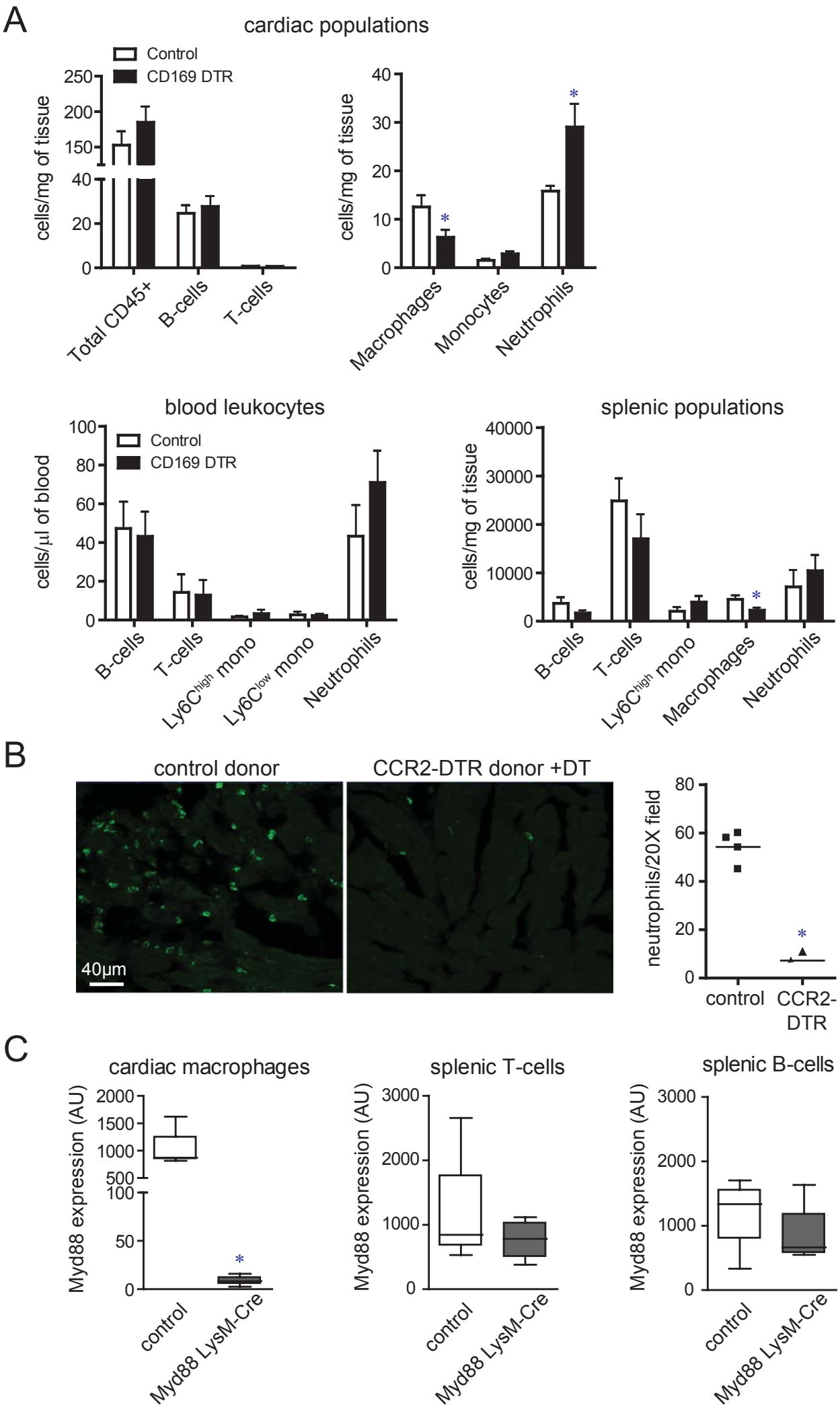
A
cardiac populations
Control
CD169 DTR
cells/mg of tissue
Total CD45+
B-cells
T-cells
Macrophages
Monocytes
Neutrophils
blood leukocytes
cells/µl of blood
splenic populations
Ly6C^high mono
Ly6C^low mono
B
control donor
CCR2-DTR donor +DT
40µm
neutrophils/20X field
control
CCR2-DTR
C
cardiac macrophages
splenic T-cells
splenic B-cells
Myd88 expression (AU)
Myd88 LysM-Cre

Online Figure V. Cardiac immune populations in CD169-DTR mice and neutrophil recruitment following cardiac transplantation. A, Quantification of flow cytometry data showing absolute numbers of B-cells, T-cells, neutrophils, monocytes, and macrophages in the heart, blood and spleen in control and CD169-DTR mice following DT administration. *$p<0.05$ compared to control. n=4 per experimental group. **B**, Ly6G immunostaining in control and CCR2-DTR donor hearts 2 days following transplantation. DT was administered to donor mice prior to transplantation. 200X magnification. Quantification of Ly6G+ neutrophils per 20X field. **C**, Quantitative RT-PCR for Myd88 mRNA in cardiac macrophages, T-cells, and B-cells isolated from control and $Myd88^{flox/flox}$ LysM-Cre mice. n=4 per experimental group. *$p<0.05$ compared to control.

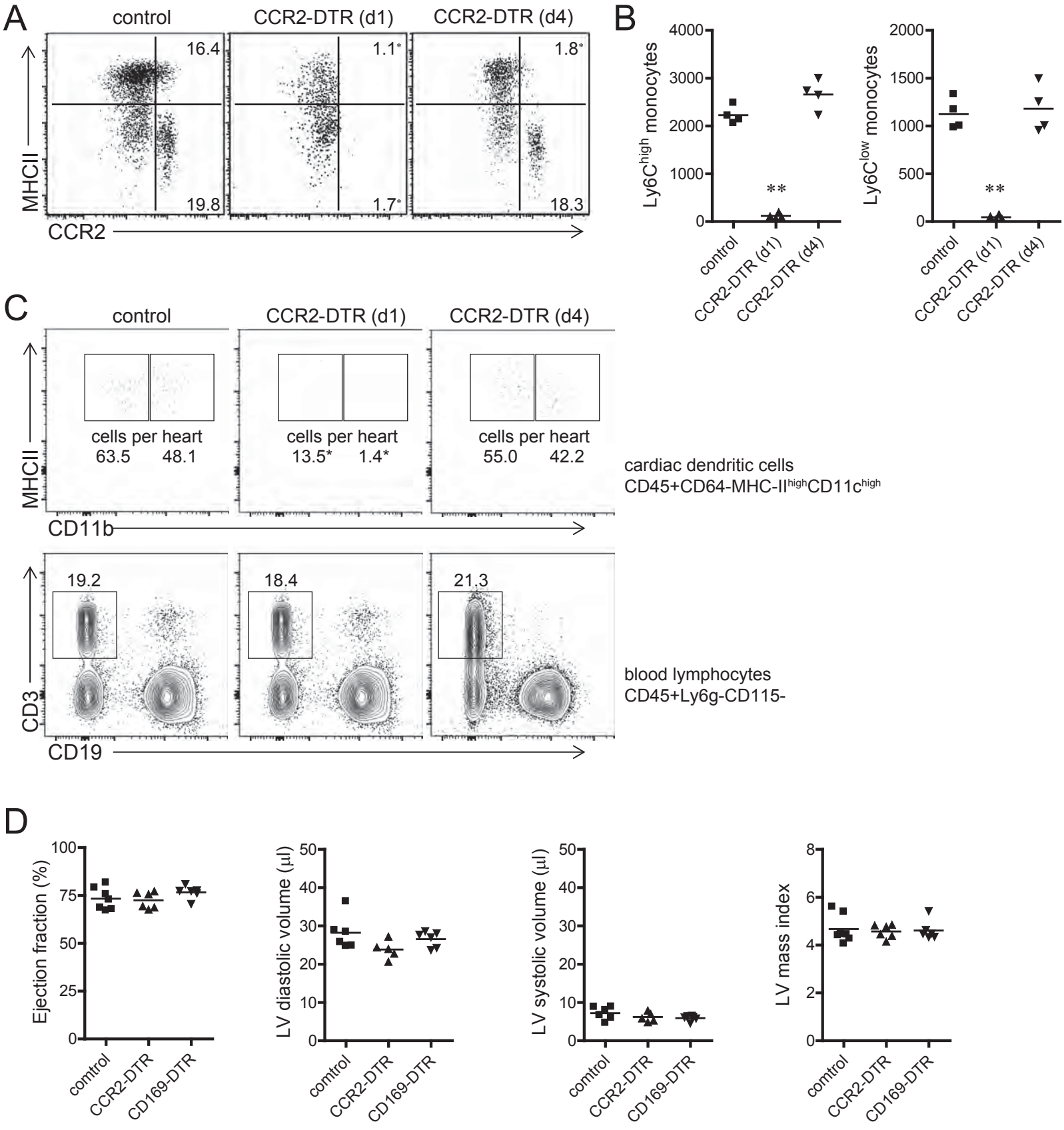
A
control
CCR2-DTR (d1)
CCR2-DTR (d4)
16.4
19.8
1.1*
1.7*
1.8*
18.3
MHCII
CCR2
B
Ly6C^high monocytes
Ly6C^low monocytes
4000
3000
2000
1000
0
2000
1500
1000
500
0
**
**
control
CCR2-DTR (d1)
CCR2-DTR (d4)
C
control
CCR2-DTR (d1)
CCR2-DTR (d4)
cells per heart
63.5 48.1
cells per heart
13.5* 1.4*
cells per heart
55.0 42.2
MHCII
CD11b
cardiac dendritic cells
CD45+CD64-MHC-II^highCD11c^high
19.2
18.4
21.3
CD3
CD19
blood lymphocytes
CD45+Ly6g-CD115-
D
Ejection fraction (%)
100
75
50
25
0
LV diastolic volume (µl)
50
40
30
20
10
0
LV systolic volume (µl)
50
40
30
20
10
0
LV mass index
8
6
4
2
0
comtrol
CCR2-DTR
CD169-DTR

Online Figure VI. Strategy to deplete resident CCR2+ macrophages prior to myocardial infarction. A, Flow cytometry of cardiac CD45+CD64+ monocytes and macrophages from control and CCR2-DTR mice. CCR2-DTR mice were administered a single dose of DT (100ng, IP) and analyzed at either day 1 (d1) or day 4 (d4) following DT injection. Values displayed indicate the percentage of MHC-II^{high}CCR2+ macrophages and MHC-II^{low}CCR2+ monocytes. *p<0.05 compared to control. **B**, Quantification of the number of peripheral blood Ly6C^{high} and Ly6C^{low} monocytes in control and CCR2-DTR experimental groups. **p<0.05 compared to all other groups. **C**, Flow cytometry of cardiac dendritic cells (CD45+CD64-MHC-II^{high}CD11^{high}) and blood lymphocytes (CD45+Ly6G-CD115-) in CCR2-DTR mice at baseline, day 1, and day 4 following DT injection. Values displayed indicate either total number of dendritic cells per heart or the percentage of blood lymphocytes. **D**, Quantification of echocardiographic data describing LV systolic function and chamber dimensions of control, CCR2-DTR, and CD169-DTR hearts following DT administration.

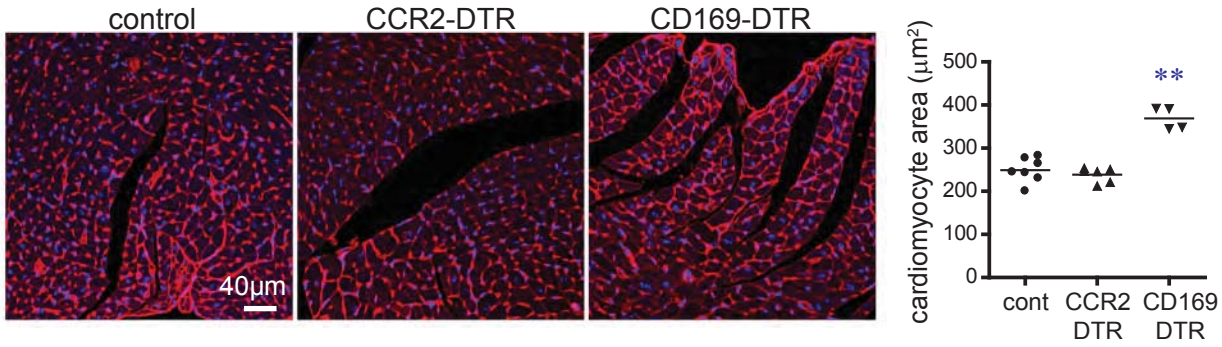
control
CCR2-DTR
CD169-DTR
40μm

cardiomyocyte area (μm²)
500
400
300
200
100
0
**
cont
CCR2 DTR
CD169 DTR

Online Figure VII. Cardiomyocyte hypertrophy in the remote zone following myocardial infarction. Left, WGA staining (red) of control, CCR2-DTR, and CD169-DTR hearts 28 days following ischemia reperfusion injury. DT was administered prior to ischemia reperfusion injury. 200X magnification. Blue: DAPI. **Right**, Quantification of cardiomyocyte cross-sectional area. **p<0.05 compared to all other groups.

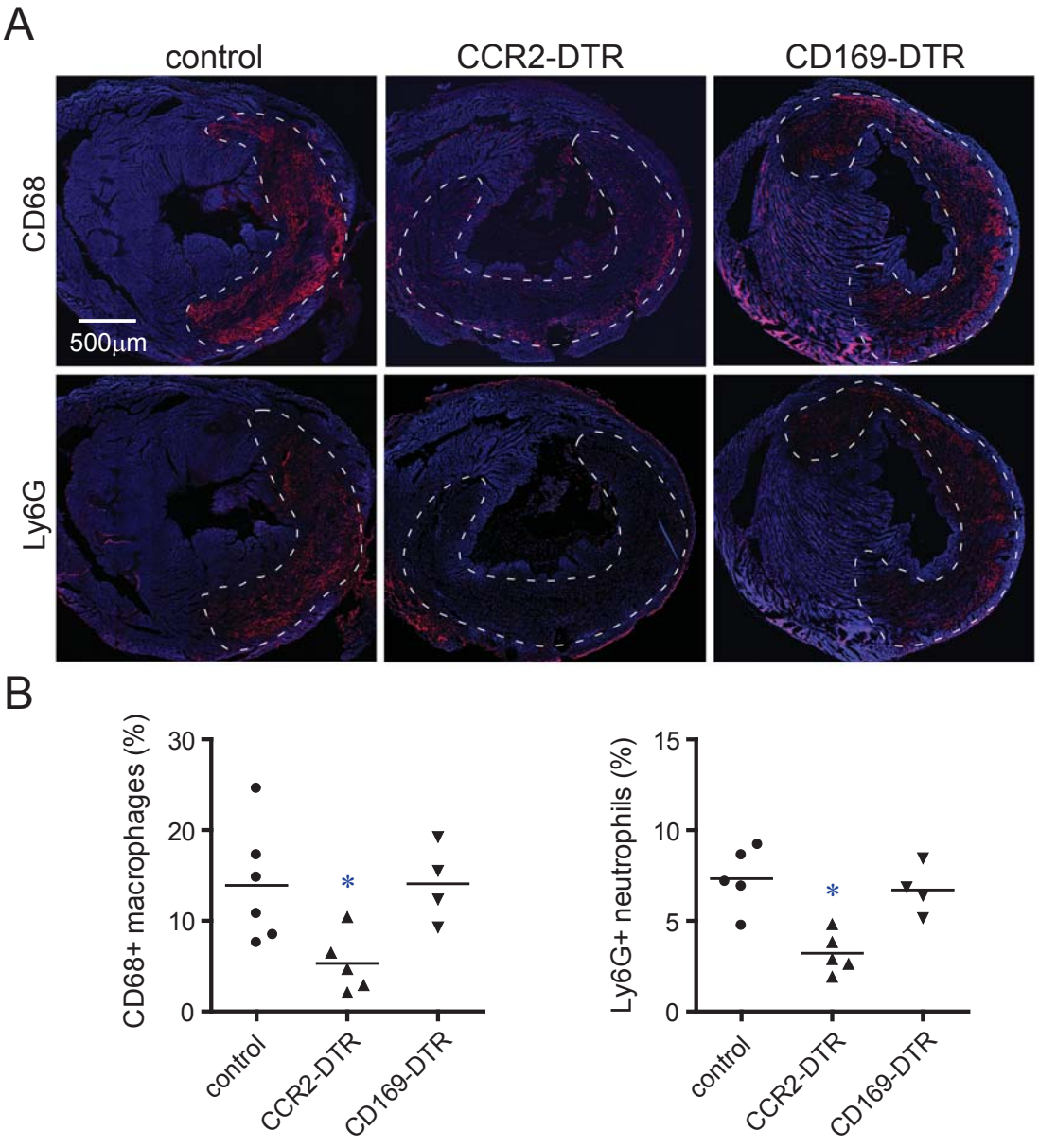
A
control
CCR2-DTR
CD169-DTR
CD68
Ly6G
500μm
B
CD68+ macrophages (%)
30
20
10
0
control
CCR2-DTR
CD169-DTR
*
Ly6G+ neutrophils (%)
15
10
5
0
control
CCR2-DTR
CD169-DTR
*

Online Figure VIII. Monocyte and macrophage abundance following myocardial infarction. A, Immunostaining for CD68 and Ly6G showing macrophage and neutrophil abundance in the infarct (white dashed lines) of control, CCR2-DTR, and CD169-DTR hearts 2 days following ischemia reperfusion injury. DT was administered prior to ischemia reperfusion injury. Tile scans of 100X magnification images. **B,** Quantification of CD68 and Ly6G signal within the infarct. Data is displayed as percentage of infarct area that is CD68 or Ly6G positive. *$p<0.05$ compared to all other groups.

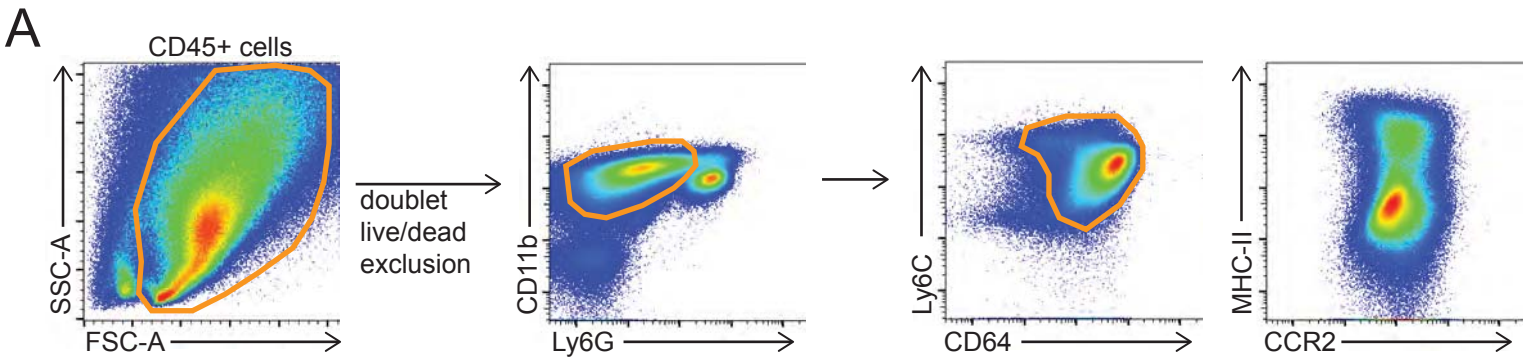
A
CD45+ cells
SSC-A
FSC-A
doublet
live/dead
exclusion
CD11b
Ly6G
Ly6C
CD64
MHC-II
CCR2

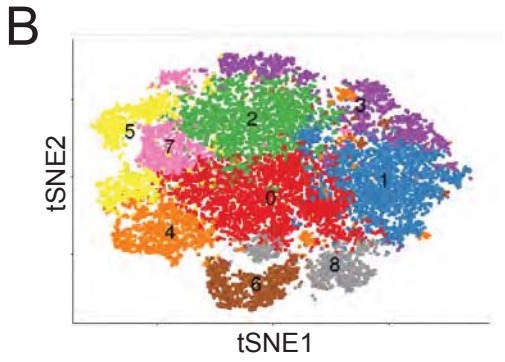
B
tSNE2
tSNE1
0
1
2
3
4
5
6
7
8

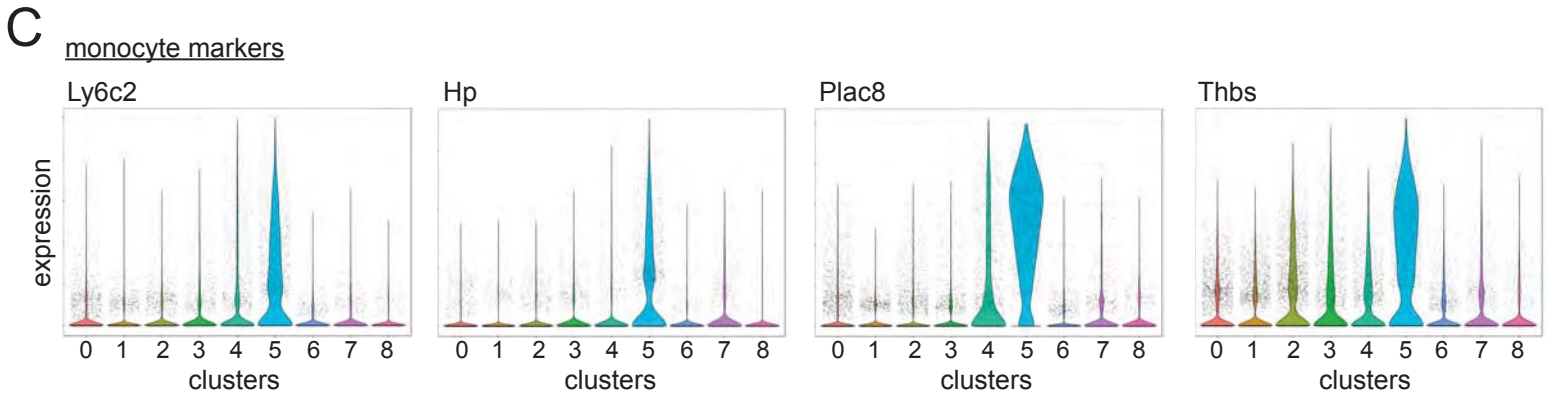
C
monocyte markers
Ly6c2
Hp
Plac8
Thbs
expression
0 1 2 3 4 5 6 7 8
clusters

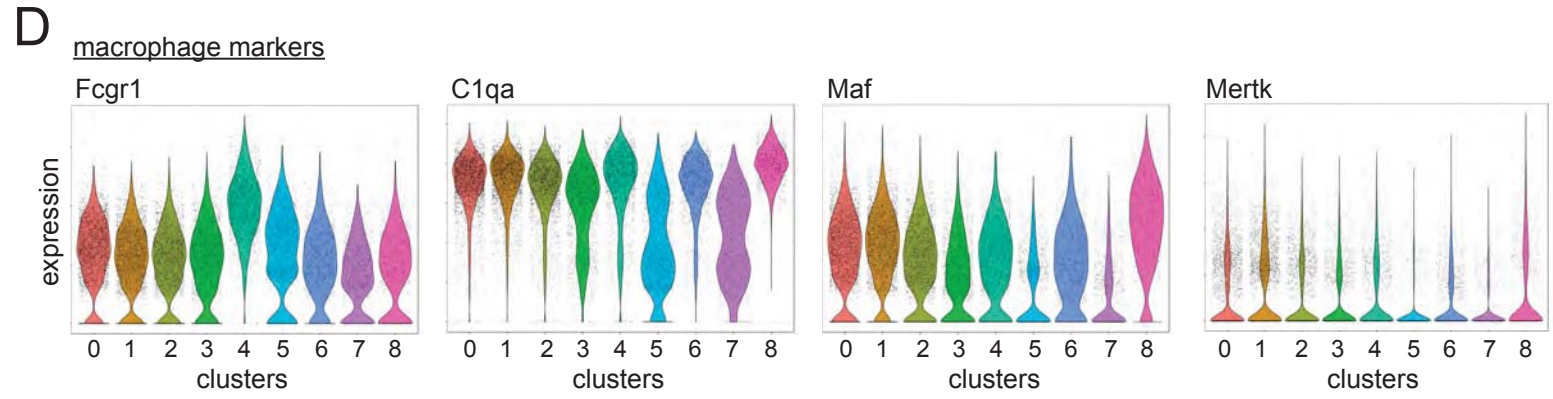
D
macrophage markers
Fcgr1
C1qa
Maf
Mertk
expression
0 1 2 3 4 5 6 7 8
clusters

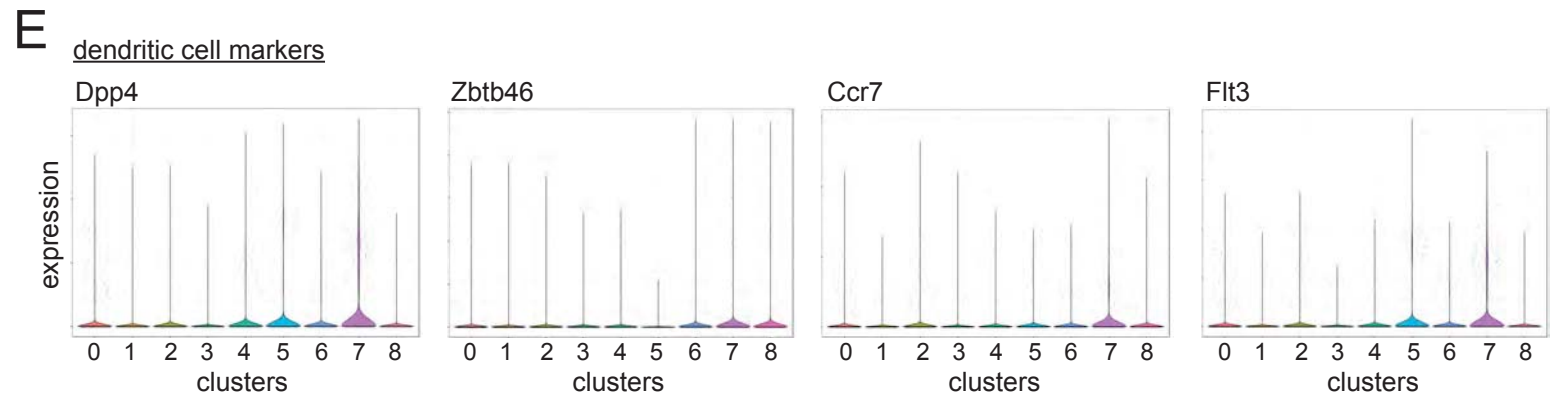
E
dendritic cell markers
Dpp4
Zbtb46
Ccr7
Flt3
expression
0 1 2 3 4 5 6 7 8
clusters

Online Figure IX. Single cell RNA sequencing of monocytes and macrophages following myocardial infarction. A, Flow cytometry gating strategy employed for the single cell RNA sequencing analyses. Final sorted population was CD45+CD11b+Ly6G-CD64+ cells. **B**, tSNE plot showing monocyte and macrophage clusters. **C**, Violin plot showing the expression of monocyte markers across clusters. **D**, Violin plot showing the expression of macrophage markers across clusters. **E**, Violin plot showing the expression of dendritic cell markers across clusters.

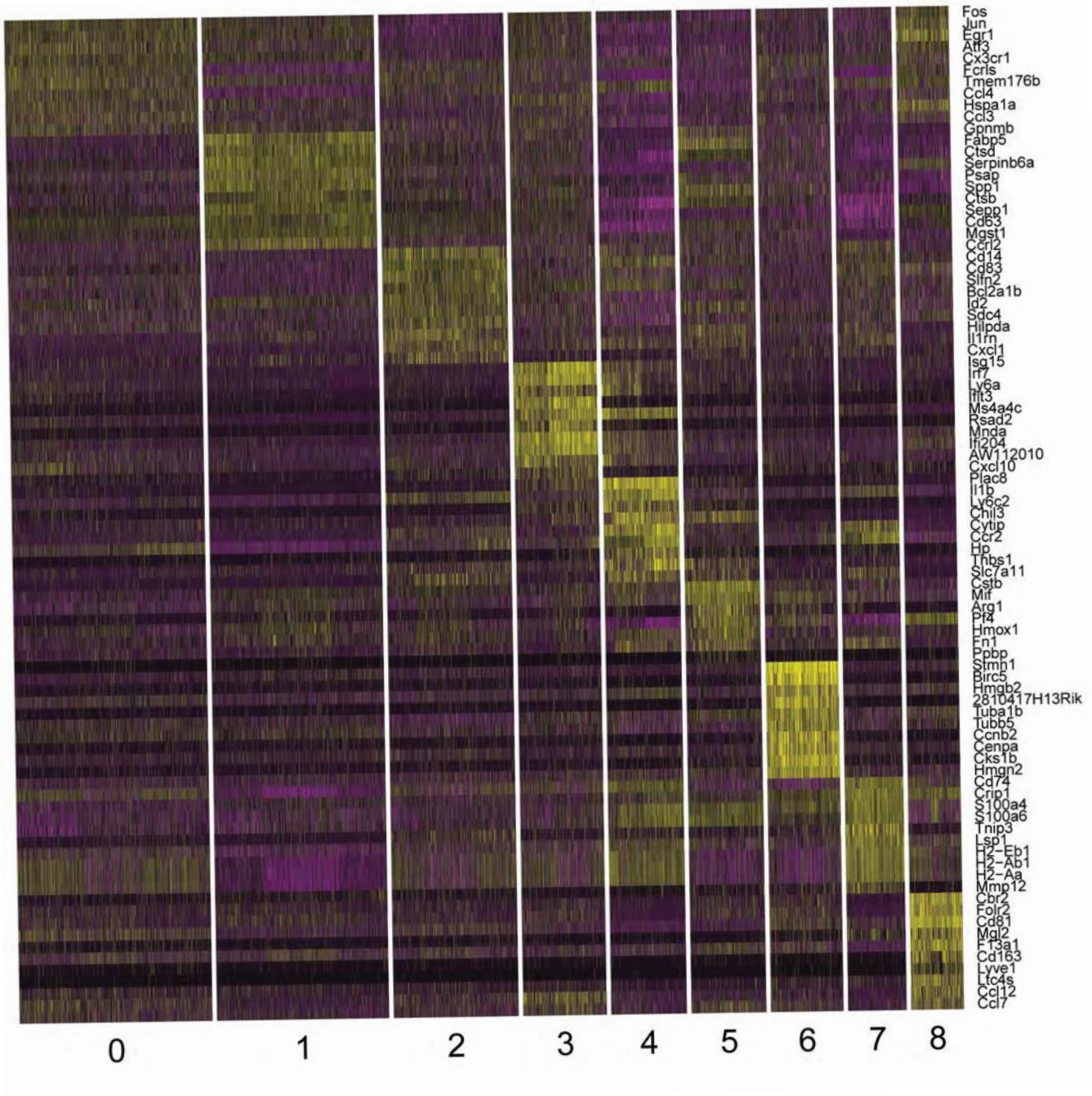
Fos
Jun
Egr1
Atf3
Cx3cr1
Fcrls
Tmem176b
Ccl4
Hspa1a
Ccl3
Gpnmb
Fabp5
Ctsd
Serpinb6a
Psap
Spp1
Ctsb
Sepp1
Cd63
Mgst1
Ccrl2
Cd14
Cd83
Slfn2
Bcl2a1b
Id2
Sdc4
Hilpda
Il1rn
Cxcl1
Isg15
Irf7
Ly6a
Ifit3
Ms4a4c
Rsad2
Mnda
Ifi204
AW112010
Cxcl10
Plac8
Il1b
Ly6c2
Chil3
Cytip
Ccr2
Hp
Thbs1
Slc7a11
Cstb
Mif
Arg1
Pf4
Hmox1
Fn1
Ppbp
Stmn1
Birc5
Hmgb2
2810417H13Rik
Tuba1b
Tubb5
Ccnb2
Cenpa
Cks1b
Hmgn2
Cd74
Crip1
S100a4
S100a6
Tnip3
Lsp1
H2-Eb1
H2-Ab1
H2-Aa
Mmp12
Cbr2
Folr2
Cd81
Mgl2
F13a1
Cd163
Lyve1
Ltc4s
Ccl12
Ccl7
0
1
2
3
4
5
6
7
8

Online Figure X. Cluster heat map. Seurat generated heat map showing the top 10 significant genes by fold expression in each cluster.

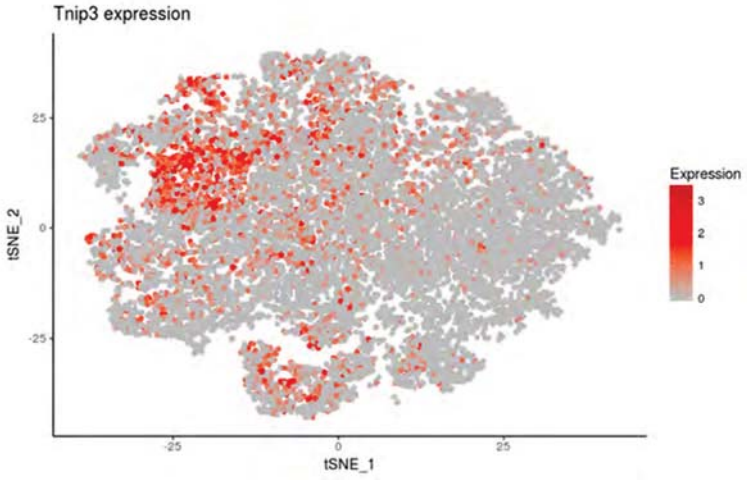
Tnip3 expression
tSNE_2
tSNE_1
Expression
3
2
1
0

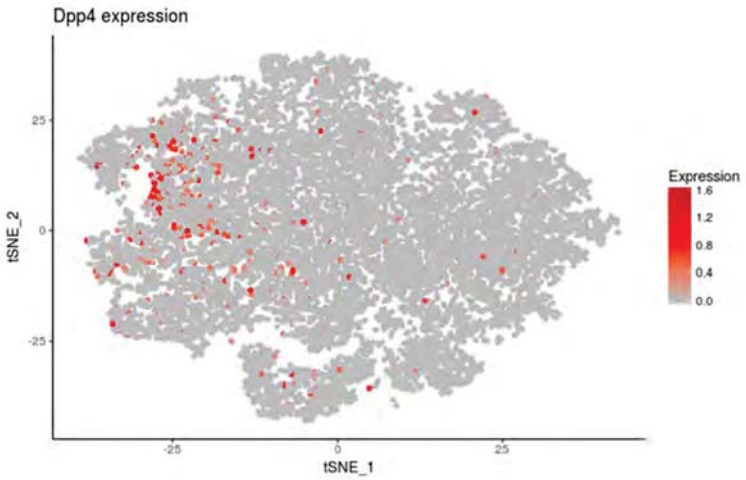
Dpp4 expression
tSNE_2
tSNE_1
Expression
1.6
1.2
0.8
0.4
0.0

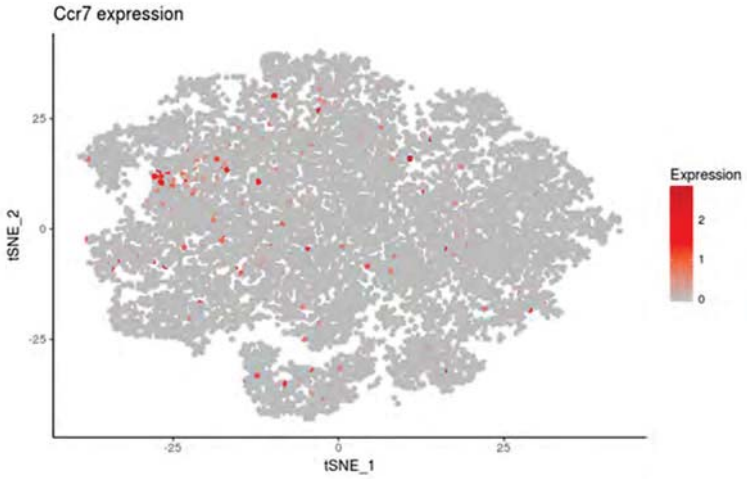
Ccr7 expression
tSNE_2
tSNE_1
Expression
2
1
0

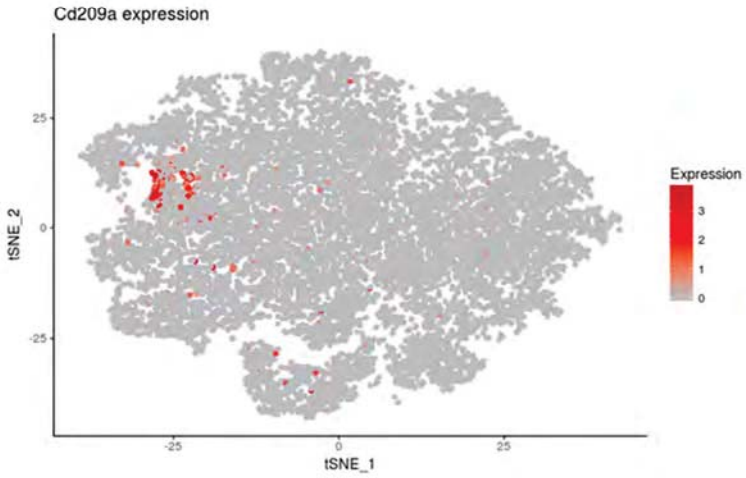
Cd209a expression
tSNE_2
tSNE_1
Expression
3
2
1
0

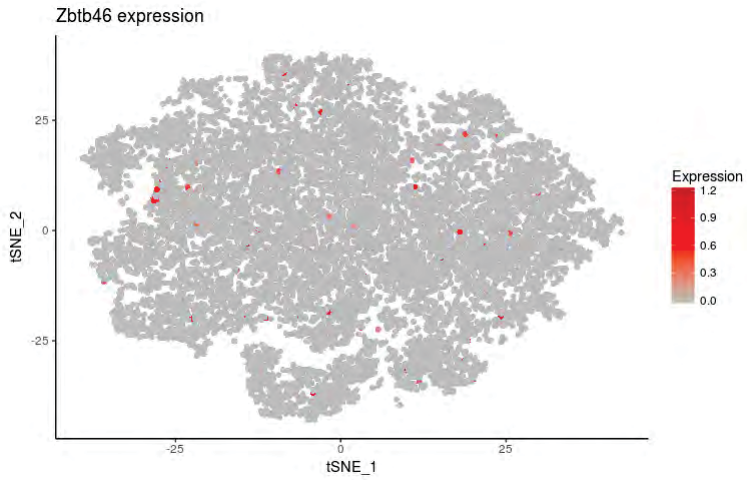
Zbtb46 expression
tSNE_2
tSNE_1
Expression
1.2
0.9
0.6
0.3
0.0

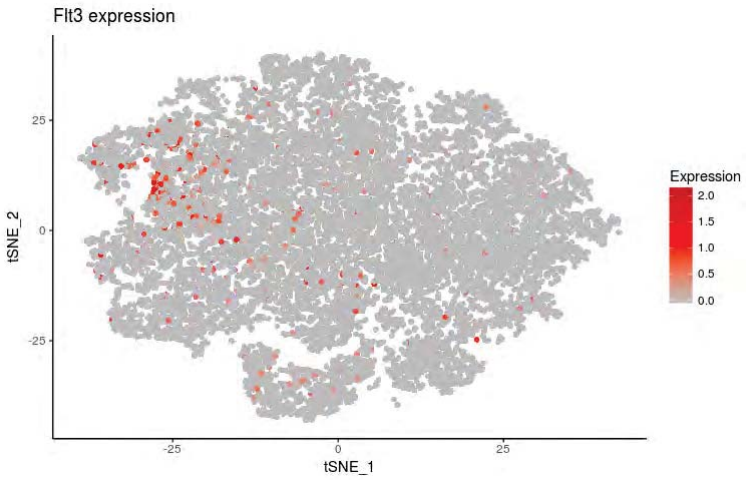
Flt3 expression
tSNE_2
tSNE_1
Expression
2.0
1.5
1.0
0.5
0.0

Online Figure XI. Dendritic cell marker expression. Feature maps showing that dendritic cell markers were expressed in a subset of cells within the Tnip3/Itgb7 cluster.

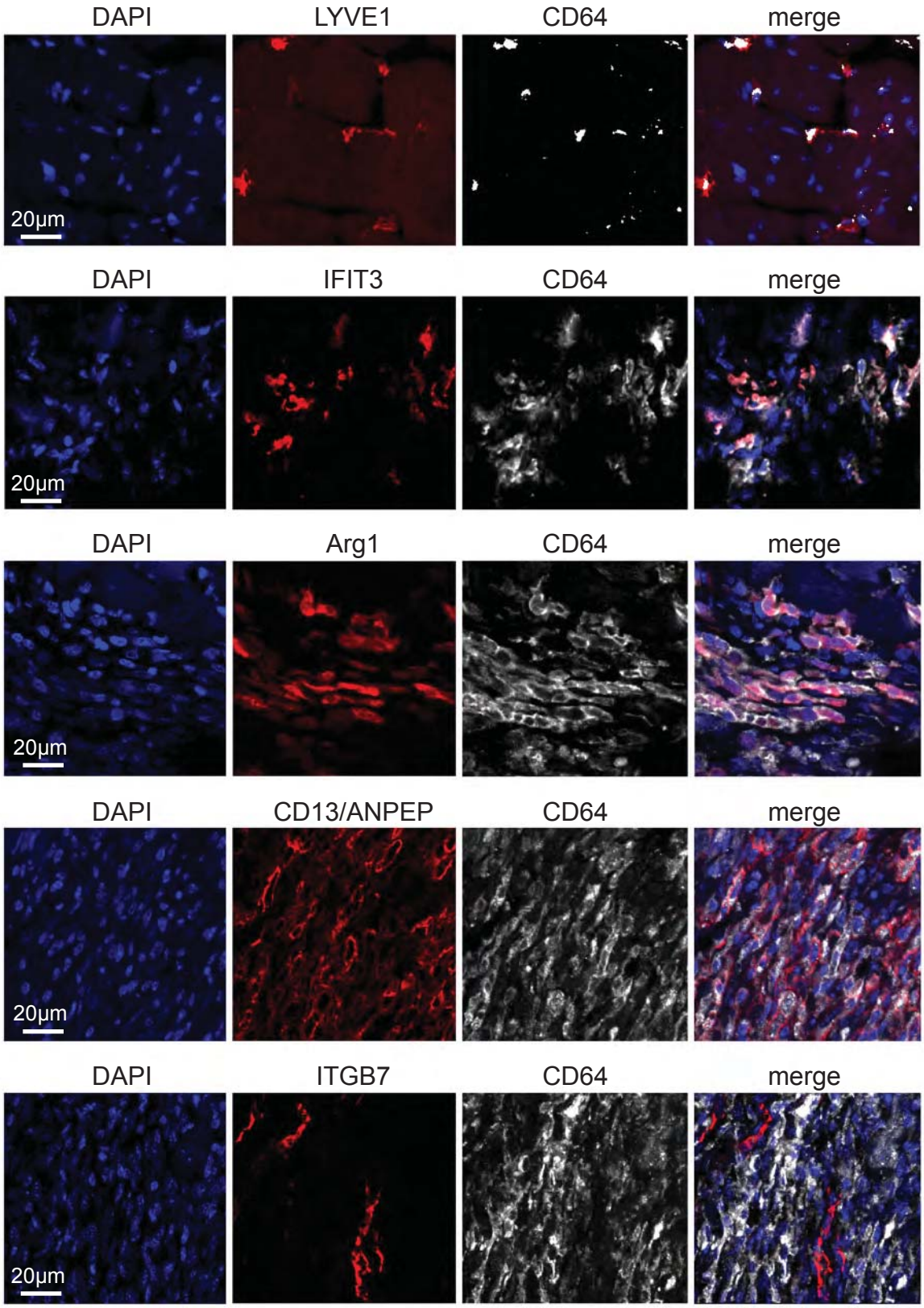
DAPI
LYVE1
CD64
merge
20μm
DAPI
IFIT3
CD64
merge
20μm
DAPI
Arg1
CD64
merge
20μm
DAPI
CD13/ANPEP
CD64
merge
20μm
DAPI
ITGB7
CD64
merge
20μm

Online Figure XII. Macrophage diversity within the infarcted heart. Immunostaining of myocardial tissue 4 days following ischemia reperfusion injury. 400X magnification images showing the morphologies of each macrophage populations.